LBL-36388
Preprint

Lawrence Berkeley Laboratory
UNIVERSITY OF CALIFORNIA

CHEMICAL SCIENCES DIVISION

Submitted to Applied Optics

Investigation of the Effects of Phase Errors on High Resolution Fourier Transform Spectroscopy of Narrow Bandwidth Spectra in the 100–200 Å Region

E.J. Moler, M. Howells, Z. Hussain, D.A. Shirley, and K.D. Möller

November 1994

Prepared for the U.S. Department of Energy under Contract Number DE-AC03-76SF00098

DISCLAIMER

LBL-36388

Investigation of the Effects of Phase Errors on High Resolution Fourier Transform Spectroscopy of Narrow Bandwidth Spectra in the 100–200 Å Region

E.J. Moler,[1] M. Howells,[2] Z. Hussain,[2] D.A. Shirley,[3] and K.D. Möller[4]

[1]Department of Chemistry, University of California and
Chemical Sciences Division, Lawrence Berkeley Laboratory,
University of California, Berkeley, California 94720

[2]Lawrence Berkeley Laboratory, Berkeley, California 94720

[3]Department of Chemistry and Physics, Pennsylvania State University,
University Park, PA 16802

[4]Department of Physics and Chemistry,
Fairleigh Dickenson University, Teaneck, NJ 07666

November 1994

This work was supported by the Director, Office of Energy Research, Office of Basic Energy Sciences, Material Sciences Division, of the U.S. Department of Energy under Contract No. DE-AC03-76SF00098.

Investigation of the Effects of Phase Errors on High Resolution Fourier Transform Spectroscopy of Narrow Bandwidth Spectra in the 100-200 Å Region

E. J. Moler[1] , M. Howells[2], Z. Hussain,[2] D. A. Shirley,[3] K. D. Möller[4]

Abstract

In considering the design and implementation of a high-resolution Fourier transform spectrometer for the soft X-ray region, it has become clear that the precision of the path length difference (phase) measurement is a critical aspect of the instrument because of constraints imposed by the short wavelengths of soft X-rays. We investigate the effects of periodic and random phase measurement errors on the frequency spectrum, derived from the Fourier transform of the interferogram, and the signal/noise ratio. Periodic phase errors lead to sidebands with positions determined by the period of the error and amplitudes that depend on the ratio of the maximum error to the wavelength. Random phase errors give rise to white noise in the frequency spectrum, with a signal/noise ratio proportional to the square root of the number of measurements and inversely proportional to the standard deviation of the measurement error .

1. Introduction

A Fourier transform spectrometer for synchrotron radiation in the 100-400 Å region is under construction at the Advanced Light Source at the Lawrence Berkeley Laboratory [1]. The design goal of the instrument is a resolving power $E/\Delta E \sim 10^6$, which will enable investigation of previously inaccessible features of the helium absorption spectrum near the double ionization threshold[2]. There are, however, technical challenges posed by the short wavelengths of soft X-rays. In particular, the precision of the path-length difference measurement is a key aspect of the instrument. This problem, while previously recognized, has not been of great concern as most Fourier transform spectroscopy has been carried out in the infra-red region, where the wavelengths are relatively long [3]. We call an error in path-length difference a "phase error" in the measurement of the interferogram. Amplitude errors, such as detector noise and photon counting statistics, have been thoroughly treated, as they are common to all forms of spectroscopy [4]. Thus, we consider only the phase error effects here. We first give a brief description of the FT-

[1] Lawrence Berkeley Laboratory and Department of Chemistry, University of California, Berkeley, Berkeley, California 94720, USA.
[2] Lawrence Berkeley Laboratory, Berkeley, California, 94720, USA
[3]Department of Chemistry and Physics, Pennsylvania State University, University Park, PA 16802, USA
[4] Department of Physics and Chemistry, Fairleigh Dickenson University, Teaneck, NJ 07666, USA

SX spectrometer and the equations used to represent the interferogram, then we discuss phase errors and their effects under the categories of constant, periodic, and random phase errors.

The FT-SX spectrometer under construction at the Lawrence Berkeley Laboratory will use, as a light source, the narrow bandwidth output of a spherical grating monochromator on a bend-magnet beam line at the Advanced Light Source. Before the detector will be a gas absorption cell containing, for example, helium. The interferogram will be sampled by moving one set of mirrors of a Mach-Zehnder interferometer continuously at a slow speed, inducing a continuously varying path-length difference (PLD) between the two arms of the beam, and recording the signal at constant position intervals. To obtain the desired resolution of 10^6 the interferogram must be very long, about 2 cm for the soft X-ray wavelength range. Additionally, the resolution of the position measurement should be a small fraction of the soft X-ray wavelength, e. g., 5-10 Å. This combination of very high resolution position-measurement and long travel distance has led us to select heterodyne laser interferometry as our position measurement method. There are commercially available systems based on this method, using a HeNe laser with a claimed resolution of <6 Å. However, certain errors, both random and periodic, are known to be associated with these devices [5]. It is our desire to understand and estimate the effects of these phase errors on the final absorption spectrum and to correct for them if necessary. The function used for the investigation of phase errors is the interferogram function for a monochromatic source,

$$S_g = \cos(\omega_g x + 2\pi\varepsilon_x) = \cos\left(\frac{2\pi}{\lambda_g}x + 2\pi\varepsilon_x\right) \quad (1)$$

where ω_g, λ_g are the frequency and wavelength of the light, x is the induced path-length difference, and ε_x is the phase error in fractions of a wavelength, and is usually dependent in some way on x. The amplitude is set to unity for convenience. The Fourier transform of this function is a delta function at frequency ω_g. The discrete form of equation 1 is,

$$S_g = \cos\left(\frac{2\pi n}{p} + 2\pi\varepsilon_n\right) \quad (2)$$

where n is the sample position index, p is the number of sample points per period of the signal, and ε_n is the phase error. Appendix A has a more complete discussion of the connection between the above equations and the meaning of their parameters. We can characterize the types of phase errors based on whether ε_n is constant, periodic, or random.

2. Case 1:ε is constant

This case corresponds to missing the zero path-length difference position, creating a sampled output signal that no longer appears even. We would point out that, in general, this results in a frequency-dependent loss of information since the odd parts of the signal near the Nyquist frequency are attenuated or lost all together. This problem, which is largely a data analysis problem, has been treated elsewhere as it is common to all Fourier transform spectroscopies [6]. We will therefore not deal with it here.

3. Case 2: ε is periodic

It is known that heterodyne interferometers suffer from periodic errors in their position measurements due to imperfect separation of the two different frequency components [5]. The period is that of the nominal wavelength of the laser light used. Thus, for a HeNe laser there is an error that has a period of 633/8 nm in translation for a four-pass plane mirror system. We may represent this error, in units of path-length distance, as

$$\mathrm{E} = \beta \sin(\omega_m x) \qquad (3)$$

then our signal becomes

$$S_g = \cos(\omega_g x + \mathrm{E}) = \cos(\omega_g x + \beta \sin(\omega_m x)) \quad (4)$$

where ω_g is the frequency of our (monochromatic) signal and ω_m is the effective frequency of the laser position indexer. The signal is thus an angle-modulated function. The maximum position measurement error is β. Because the mirrors are arranged for grazing reflections of the soft X-rays, there is a geometric factor relating the movement of the mirrors and the path-length difference introduced. This factor, along with the optical arrangement of the laser position transducer, leads to an "effective" period when compared to the soft X-rays. We show in appendix B that this function is equivalent to

$$\begin{aligned} S_g &= \sum_t J_t(\beta)(-1)^t \left[\cos\left((\omega_g - t\omega_m)x\right) - \cos\left((\omega_g + t\omega_m)x\right)\right] \\ &= J_0(\beta)\cos(\omega_g x) \\ &\quad - J_1(\beta)\left[\cos\left((\omega_g - \omega_m)x\right) - \cos\left((\omega_g + \omega_m)x\right)\right] \\ &\quad + J_2(\beta)\left[\cos\left((\omega_g - 2\omega_m)x\right) - \cos\left((\omega_g + 2\omega_m)x\right)\right] \\ &\quad - J_3(\beta)\left[\cos\left((\omega_g - 3\omega_m)x\right) - \cos\left((\omega_g + 3\omega_m)x\right)\right] \\ &\quad + \cdots \end{aligned} \qquad (5)$$

where the J's are Bessel functions of the first kind [7]. Thus the result is a set of symmetrically spaced sidebands (ghosts) about the real signal at multiples of the modulation frequency. The amplitude of the modulation function (the maximum error in path-length difference) determines the amplitudes of the sidebands. The larger the

modulations, the more sidebands that become apparent. With no modulation , $\beta = 0$, the formula reduces to a single frequency at the original signal peak, as expected. For small modulations only the first sideband has a non-negligible intensity. The total power in the spectrum

$$J_0^2(\beta) + 2\sum_t J_t^2(\beta) = \frac{1}{2} \qquad (6)$$

is constant. So with a periodic angular modulation (position measurement error), power is removed from the main peak and appears in the sidebands. All of these sidebands scale with the intensity of the signal. One should note that, although the main signal loses power, any multiplicative noise will, in general, not be reduced. Thus one loses signal/noise with this kind of phase error.

To make use of the above results and apply them to the case of position measurement error in Fourier transform spectrometry, we write the position as,

$$x \rightarrow x + \beta \sin\left(\frac{2\pi x}{\lambda_m}\right) \qquad (7)$$

and have for the signal,

$$\begin{aligned} S_g &= \cos\left[\left(\frac{2\pi}{\lambda_g}\right)\left(x + \beta\sin\left(\frac{2\pi x}{\lambda_m}\right)\right)\right] = \cos\left[\frac{2\pi x}{\lambda_g} + \frac{2\pi\beta}{\lambda_g}\sin\left(\frac{2\pi x}{\lambda_m}\right)\right] \\ &= J_0(2\pi\beta')\cos\left(\frac{2\pi x}{\lambda_g}\right) \\ &\quad - J_1(2\pi\beta')\left[\cos\left(\left(\frac{1}{\lambda_g} - \frac{1}{\lambda_m}\right)2\pi x\right) - \cos\left(\left(\frac{1}{\lambda_g} + \frac{1}{\lambda_m}\right)2\pi x\right)\right] \\ &\quad + J_2(2\pi\beta')\left[\cos\left(\left(\frac{1}{\lambda_g} - \frac{2}{\lambda_m}\right)2\pi x\right) - \cos\left(\left(\frac{1}{\lambda_g} + \frac{2}{\lambda_m}\right)2\pi x\right)\right] \\ &\quad - \cdots \end{aligned} \qquad (8)$$

$$\beta' = \frac{\beta}{\lambda_g} \qquad (9)$$

It is important to notice that the amplitudes of the peak and sidebands are in general dependent on the ratio of the modulation amplitude (maximum position error) to the wavelength of the spectral component of interest. Figure 1 plots the amplitudes of the main peak (normalized to 1 at zero modulation) and first sideband versus of the fractional deviation β' as written above. From the figure, an error of ±5% of the wavelength reduces the main peak amplitude has dropped by 2% (5% of the power is lost to the sidebands). At ±10% the amplitude has dropped by 10% and the first sidebands have risen to 30% of the amplitude of the main peak. Now we need to consider two questions

regarding the performance of the FT-SX interferometer: a) where are the sidebands most likely to be, and b) what are tolerable periodic errors of the position measurement system?

To answer the first question we must determine the effective period, λ_m, of the laser position transducer. From the geometry of the instrument, the wavelength of the HeNe, and the four-pass optics layout, we find that the position error is equivalent to a 58 nm modulation period. This means that the "ghosts" will appear in the Fourier transform spectrum at ±21 eV from the real signal. This is quite far out of the range of the bandwidth of the incoming light (~1% at 65 eV). Therefore, the only effect on the final spectrum will be to reduce the signal-to-noise ratio, provided that precautions are taken to ensure there is no aliasing of the ghosts back into the spectrum.

To answer the second question we need to consider the amplitude of the periodic measurement errors. Our criteria for evaluating acceptable intensity loss of the signal is to try to keep the loss of the same order as the photon shot noise level in the spectrum. For a signal/noise amplitude ratio of 300, as estimated for the FT-SX [1] for a single scan, this would entail an amplitude loss to 0.9967 or only 0.33%. Making use of the limiting relation when $\beta' << 1$ for the zeroeth order Bessel function

$$J_0 \cong 1 - \left(\frac{\beta'}{2}\right)^2$$
$$\beta' \cong 2\sqrt{1 - J_0} \qquad (10)$$

Plugging in 1/300 for $1 - J_0$ gives a PLD error of β'=0.115 and, again using the geometric factors of the instrument, we get a position measurement fractional error of 5.8%. For the nominal wavelength of 200 Å this becomes ±12 Å of error. This is a realistic goal and should be achievable with the laser interferometer. To operate at higher energies requires even tighter tolerances. At 100 Å (120 eV) the allowed error of 6 Å becomes more challenging. With a fractional error of 10% of the xray wavelength we still lose only 10% of the signal amplitude.

4. Case 3: ε is random

The effects of random errors in the sample position become important when the resolution of the position measurement system is comparable to the wavelengths of light passing through the instrument. In particular, the heterodyne laser interferometer has a noise component in the output due to variations in air density in the laser path, noise in the measurement electronics, etc. Heuristically speaking, one would expect such noise to generate many ghosts in the final spectrum. This can be understood from the results of the investigation of periodic errors discussed above and from the statistical properties of a noise wave form (see appendix C). We would expect the distribution of noise in the final

(energy) spectrum to be white (each a ghost from one spectral component of the modulating noise) with magnitudes following a Rayleigh distribution.
In order to asses the effect of such phase noise on the final Fourier-transform spectrum, numerical simulations have been carried out. We begin again with the relation

$$S_g = \cos\left(\frac{2\pi n}{p} + 2\pi\varepsilon_n\right) \qquad (11)$$

and let ε_n vary randomly from one sample point to the next. The probability distribution used to generate the error term is gaussian with zero mean obtained from an integer distribution with $2^{32}-2$ values using the Central Limit Theorem with 12 samples [8]. Note that the units of the error term ε_n is in fractions of the monochromatic signal's wavelength. The interferograms were generated by "sampling" the function, assuming equally spaced intervals, but allowing the error term to modify the value obtained in that sample. The amplitude signal to noise ratio (S/N) were estimated for each interferogram. The signal amplitude was estimated by taking the total intensity under the "peak" in the fast Fourier transform (FFT) and subtracting the mean intensity of the noise away from the peak. The standard deviation of the spectral components away from the peak were calculated using a large number of their magnitudes. The ratio of the two is the S/N. For example, figure 2 shows 5 periods of a g=256 period interferogram with p=8 points/period and a noise standard deviation of 0.100. Also shown is the zero noise function for comparison. The Fourier transforms of those two interferograms are shown as well. The general feature to be noticed is that the spectrum of the interferogram with phase noise shows a reduction in peak intensity and a distribution of noise components across the entire frequency spectrum (the full range of the FFT is not shown in the figure). A histogram of the noise amplitudes from the above Fourier transforms, shown in figure 3, confirms our expectation regarding the statistical distribution of the noise amplitudes. The three parameters, p (number of samples/period), g (total periods included in sample set), and σ (standard deviation of gaussian noise) of ε_n, were varied independently while holding the other two constant in order to ascertain their effect on the Fourier transform. The number of sample points per period, p, was varied from 2 to 64. The number of periods of the signal included in an interferogram, g, were varied from 64 to 256 and the rms value of the phase noise was varied from 0.001 to 0.5. The latter number can be understood as the standard deviation of the position error being $\pm 1/2$ period. As discussed in the Appendix A, the equations and parameters are defined such that the frequency scale is normalized to the main signal, which always appears at 1/2 Hz. Figure 4 shows the magnitudes of the FFT's of three interferograms in which the noise σ was 0.01, 0.1, and 0.3. The number of samples per period, p, is 4 and the total number of

periods included, g, is 256. Shown in each figure is the estimated signal to noise amplitude ratio for these spectra. The results of these simulations can be summarized as follows:

$$\frac{S}{N} \propto \frac{1}{\sigma}, \quad \text{for } \sigma \leq 0.1$$
$$\frac{S}{N} \propto \sqrt{p} \qquad (12)$$
$$\frac{S}{N} \propto \sqrt{g}$$

Putting all of these together we get

$$\frac{S}{N} = c\frac{\sqrt{pg}}{\sigma} = \frac{\sqrt{N}}{4\sigma} \qquad (13)$$

and we find that the signal to noise ratio varies inversely with the increase in position noise and directly with the square root of the total number of observations, which, in retrospect, is not surprising. "c" is just a constant of proportionality which we find to be about 1/4. The trends stated above deteriorate for larger position measurement errors as the peak gets completely washed out in the noise. Also, for the Nyquist sample rate, p=2, the signal to noise is a little higher than indicated by the trend above since the derivative of the signal is zero at the crests and troughs. Of course, since real spectra are not delta functions, the values for larger sampling rates probably extrapolate back to 2 since one is probably not always sampling at the extrema. It is interesting to note that the peak positions and line shapes are not affected beyond that of the addition of random noise, as shown in figure 5. What these results mean is that one overcomes the effects of noise in the sample position by increasing the sample rate until the bandwidth of the position measurement noise is exceeded. This sets the maximum necessary sampling rate of the system until the other sources of noise, e.g. detector or photon shot noise, become dominant. The benefit in signal to noise is still realized even if a filter is applied to the over sampled signal and then decimated back to the necessary sample rate. Practically speaking, for ultra-high resolution spectra where ~10^6 periods are included, the minimum number of data points is 2,000,000. An σ of 0.1 (~10 Å for the FT-SX) still gives a S/N contribution of ~3000 which is insignificant compared to the expected contributions from the photon shot noise. For broad bandwidth studies, though, the benefit may be more important since most of the information is contained in a relatively narrow region around the zero PLD. Sampling at PLD's beyond which the oscillations have died out do not count.

5. Conclusions

The effects of phase errors in the interferogram on the Fourier-transformed energy spectrum have been studied. These errors are critical when working in the soft X-ray range where the wavelengths are comparable to the resolution of the mirror position measurement system. The main effect of both periodic and random phase errors is to reduce the main signal amplitude. Periodic errors in the position measurement system generate "ghosts", sidebands to either side of the signal which appear at integral multiples of the modulation frequency. The loss of signal amplitude from the main signal depends on the ratio of the amplitude of the position measurement error and the wavelength of the signal. The "true" signal's amplitude goes as the zeroeth order Bessel function of this ratio. For the Fourier transform spectrometer under construction at the Advanced Light Source, we expect the ghosts to appear at ± 21 eV. With a position measurement error amplitude of 10% (~11 Å at 200Å wavelength region) we expect a loss of signal, and therefore of signal/noise, of 10%. Random phase errors lead to a signal to noise ratio that goes up with the square root of the total number of samples. The signal loss, like the periodic error case, depends on the ratio of wavelength to rms error. For the FT-SX spectrometer an rms of 10% of the nominal wavelength will not contribute significantly to the signal to noise ratio of a single, high resolution scan.

Appendix A: The Interferogram Function

We now discuss the functions and notations used for the discussion and simulations and the various interpretations that can be applied to understand what they mean. The output signal of an interferometer is given by

$$I(x) = \frac{I_0}{2}\left(1 + \int B(\gamma)\cos(2\pi\gamma x)\,d\gamma\right) \quad (A1)$$

The oscillatory part of the signal contains the spectral information. We write this interferogram function as

$$S(x) = \int B(\gamma)\cos(2\pi\gamma x)\,d\gamma \quad (A2)$$

where $\gamma = 1/\lambda$ is the wave number, x is the path length (phase) difference between the two beams in the interferometer, and $B(\gamma)$ is the spectral distribution of the signal. If the function is of finite length ΔL it can be uniquely resolved into a sum of discrete cosines and sines with frequencies which are integral multiples of the resolution $\delta\gamma = 1/2\Delta L$. We will only consider the even (real) functions in S here and thus write

$$S(x) = \sum_{k=1}^{\frac{\Delta L}{2}} b_k \cos\left(\frac{2\pi k}{\Delta L}x\right) \quad (A3)$$

where k is the frequency index (*not* the wave vector). For simplicity and clarity we will assume that the spectral amplitudes, b_k, are unity. If we sample this function at intervals δl then we can write

$$S(n) = \sum_{k=1}^{\frac{\Delta L}{2}} \cos\left(\frac{2\pi k}{\Delta L} n\delta l\right) \qquad (A4)$$

The run of a single frequency component of this function is written as

$$S_k = \cos\left(\frac{2\pi k}{\Delta L} n\delta l\right) \qquad (A5)$$

where the dependence on n is implicit. Since $\Delta L / \delta l$ is the total number of points, which we call N, we arrive at yet another form of the function which is commonly used when discussing FTS,

$$S_k = \cos\left(\frac{2\pi kn}{N}\right); \quad n = 1,2,\ldots,N \qquad (A6)$$

To summarize what we have so far:

N	is the total number of sample points
n	is the sample position index
k	is the frequency index

We find it convenient to introduce two new parameters which provide a more natural scale for illustrating the various effects of errors, p and g, particularly when we are only considering a single frequency, i.e. an ideally monochromatic source. First we introduce these parameters, then describe how they are related to the other parameters and discuss their interpretation. We define the total number of points to be

$$N = pg \qquad (A7)$$

thus

$$k = 1,2,\ldots,\frac{pg}{2} \qquad (A8)$$

Then we can write the signal as

$$S_k = \cos\left(\frac{2\pi kn}{pg}\right) \qquad (A9)$$

We take our signal of interest to be a single spectral component of frequency $k = g$. Then we can write, for our principle signal,

$$S_g = \cos\left(\frac{2\pi gn}{pg}\right) = \cos\left(\frac{2\pi n}{p}\right) \qquad (A10)$$

Because we have tied the total number of points to g and p, we can now consider g to be the number of periods of our signal which are included in our data set (the sample range)

and p is the number of points/period (the sample rate). Looking at the previous equation one can see that every time n is a multiple of p the function has gone through one cycle. In addition, we define the frequency scale of the transform such that

$$\delta f = \frac{1}{2g} \qquad (A11)$$

so that at our signal frequency

$$k\delta f = \frac{g}{2g} = \frac{1}{2} \qquad (A12)$$

hence our signal always has a frequency of 1/2 Hz in this scale, independent of the sample rate p or the total number of periods g included. We also find that the total frequency range of the transform is

$$\Delta f = k_{\max}\delta f = \frac{pg}{2} \times \frac{1}{2g} = \frac{p}{4} \quad (A13)$$

So at the Nyquist sampling rate, $p = 2$, we find $\Delta f = 1/2$, i.e. our signal peak comes at the last channel of the transform. Naturally, increasing the sampling rate increases the frequency range of the transform, but the signal peak remains at $1/2$. Also, increasing the number of periods included in the data range improves the resolution of the transform. To summarize our parameters,

p	is the number of points/period of our signal,
g	is the number of periods included in the data range(or frequency),
$N = pg$	is the total number of points sampled,
$n = 1 \ldots N$	is the sample position index,
$k = 1 \ldots \frac{pg}{2}$	is the frequency index, and
$S_g = \cos\left(\frac{2\pi n}{p}\right)$	is the sampled output of the detector. The signal amplitude is assumed to be one.

When dealing with only the signal frequency, there is another approach to arrive at the above expression. Backing up a few steps, but considering a monochromatic signal of wavelength $\lambda = 1/\gamma$, we can write

$$S_g = \cos\left[\left(\frac{2\pi}{\lambda}\right)n\delta l\right] \quad (A14)$$

where δl is, again, the sampling interval. If we write δl in terms of the wavelength and the number of samples per wavelength $\delta l = \lambda / p$ then

$$S_g = \cos\left[\left(\frac{2\pi}{\lambda}\right)n\left(\frac{\lambda}{p}\right)\right] = \cos\left(\frac{2\pi n}{p}\right) \quad (A15)$$

We now have an ideal signal function to which we can introduce errors for the purpose of determining their effect on the final spectrum.

Appendix B: Derivation of the Angle-Modulated Cosine Function

We derive the spectral form of an angle-modulated cosine. This corresponds to a periodic position measurement error in a sampled interferogram. If the modulation function (position measurement function) is

$$\mathrm{E} = \beta \sin(\omega_m x) \qquad (B1)$$

then the signal becomes

$$S_g = \cos(\omega_g x + \mathrm{E}) = \cos(\omega_g x + \beta \sin(\omega_m x)) \quad (B2)$$

where ω_g is the frequency of the (monochromatic) signal and ω_m is the effective frequency of the position indexer. The maximum position measurement error is β. We will now derive an equivalent expression for this function that shows the harmonic content of the Fourier transform following Taub and Schilling [9]. Using

$$\cos(a+b) = \cos(a)\cos(b) + \sin(a)\sin(b) \qquad (B3)$$

we get

$$S_g = \cos(\omega_g)\cos(\beta \sin(\omega_m)) - \sin(\omega_g)\sin(\beta \sin(\omega_m)) \qquad (B4)$$

Now the cosine-of-sine and sine-of-sine terms can be expanded as,

$$\begin{aligned} \cos(\beta \sin(\omega_m x)) &= J_0(\beta) + 2\sum_{t=1}^{\infty} J_{2t}(\beta)\cos(2t\omega_m x) \\ \sin(\beta \sin(\omega_m x)) &= 2\sum_{t=0}^{\infty} J_{2t+1}(\beta)\cos(2t\omega_m x) \end{aligned} \qquad (B5)$$

where the J's are Bessel functions of the first kind [7]. Substituting the previous two relationships back into the expansion and using standard trigonometry identities for the products of cosines and sines we get

$$\begin{aligned} S_g &= \sum_t J_t(\beta)(-1)^t \left[\cos((\omega_g - t\omega_m)x) - \cos((\omega_g + t\omega_m)x)\right] \\ &= J_0(\beta)\cos(\omega_g x) \\ &\quad - J_1(\beta)\left[\cos((\omega_g - \omega_m)x) - \cos((\omega_g + \omega_m)x)\right] \\ &\quad + J_2(\beta)\left[\cos((\omega_g - 2\omega_m)x) - \cos((\omega_g + 2\omega_m)x)\right] \\ &\quad - J_3(\beta)\left[\cos((\omega_g - 3\omega_m)x) - \cos((\omega_g + 3\omega_m)x)\right] \\ &\quad + \cdots \end{aligned} \qquad (B6)$$

Thus the result is a set of symmetrically spaced sidebands (ghosts) about the real signal at multiples of the modulation frequency. The amplitude of the modulating wave determines the amplitudes of the sidebands.

Appendix C: Spectral Content of a Random Noise Wave form

We now discuss the harmonic content of a noise wave form. A finite length, sampled noise wave form can always be written as a sum of sines and cosines

$$\begin{aligned}\varepsilon_n &= \sum_k a_k \cos(2\pi k\,\delta f\, n) + b_k \sin(2\pi k\,\delta f\, n) \\ &= \sum_k a_k \cos\left(\frac{2\pi k n}{2p}\right) + b_k \sin\left(\frac{2\pi k n}{2p}\right) \qquad (C1) \\ &= \sum_k c_k \cos\left(\frac{2\pi k n}{2p} + \theta_k\right)\end{aligned}$$

and because the noise is a random, stationary process, the spectral amplitudes of the noise, the a_k, b_k, c_k and θ_k's, are also random variables which have statistically definable properties [Taub, p. 322]. It can be shown that the complimentary spectral amplitudes a_k, b_k or c_k, θ_k are uncorrelated with each other and uncorrelated with other spectral amplitudes. The amplitudes a_k, b_k have gaussian distributions with zero mean. In a Fourier transform one usually is interested in the magnitudes and phases, c_k, θ_k. These are related to the amplitudes a_k, b_k in the same manner that random variables in polar coordinates are related to random variables in Cartesian coordinates [Taub, p. 323]. Thus the probability distribution of the magnitude is a Rayleigh probability function

$$p(c_k) = \frac{c_k}{\Gamma} \exp\left(-c_k^2 / 2\Gamma^2\right) \qquad (C2)$$

(with the same variance as the Cartesian variables) and the phase angle has a uniform probability distribution of $1/2\pi$. Making use of the low modulation limit for the sideband amplitude of a phase modulated signal

$$J_1 \cong \frac{\beta}{2} \qquad (C3)$$

we would expect the distribution of noise in the final, sampled spectrum to be white (each a ghost from one spectral component of the noise) with magnitudes following a Rayleigh distribution.

This work was supported by the Director, Office of Energy Research, Office of Basic Energy Sciences, Material Sciences Division of the U.S. Department of Energy, under contract DE-AC03-76SF00098.

References

1. M.R. Howells, K. Frank, Z. Hussain, E.J. Moler, T. Reich, D. Moller and D.A. Shirley, "Toward a soft X-ray Fourier-transform spectrometer,"*Nuclear Instruments and Methods in Physics Research A* **347**, 182-191 (1994).

2. M. Domke, C. Xue, A. Puschman, T. Mandel, E. Hudson, D.A. Shirley, G. Kaindl, C.H. Greene and G.R. Sadeghpour, "Extensive Double-Excitation States in Atomic Helium,"*Physical Reveiw Letters* **66**, 3441-3443 (1991).

3. J. Chamberlain, The Principles of Interferometric Spectroscopy, (John Wiley and Sons, Chichester, 1979).

4. J.W. Brault, "Fourier Transform Spectrometry," in *High Resolution in Astronomy,* A. Benz, M. Huber and M. Mayer, eds., 1 Geneva Observatory, Sauverny, Switerland, 1985).

5. W. Hou and G. Wilkening, "Heterodyne interferometry errors,"*Precision Engineering* 91-98 (1992).

6. M.L. Forman, W.H. Steel and G.A. Vanasse, "Correction of Asymmetric Interferograms Obtained in Fourier Transform Spectroscopy,"*Journal of Optical Society of America* **56**, 59-63 (1966).

7. I.S. Gradshteyn and I.M. Ryzhik, Table of Integrals, Series, and Products, 973-980 (Academic Press, San Francisco, 1980).

8. W.H. Press, B.F. Flannary, S.A. Teukolsky and W.T. Vetterling, Numerical Recipes in C, (Cambridge University Press, New York, 1990).

9. H. Taub and D.L. Schilling, Principles of Communication Systems, (McGraw-Hill, San Francisco, 1986).

Figure Captions

Figure 1: Main peak and 1st side-band magnitudes vs. amplitude of periodic position error. The effect of periodic position errors is to create sidebands of each peak whose magnitudes vary with the maximum position error. As illustrated, an error of 10% of the wavelength of the main line leads to a 10% loss in amplitude to the side bands.

Figure 2: Interferograms, with and without position noise in sampling, and their FFT's. The sample rate is 8 points/period and 256 periods were included (but not shown).

Figure 3: Histogram of noise amplitudes in the FFT. The solid line is a Rayleigh distribution, which fits as expected.

Figure 4: Simulated spectra with random position errors (σ) of 0.01, 0.1, and 0.3 of a period. Included are 256 periods with a sampling rate of 4 points/cycle. The signal/noise amplitude ratio is shown for each (see text for calculation method).

Figure 5: Interferogram of 5 component "peak" with noise and its FFT. Only the envelope of the interferogram is visible. The lineshape in the FFT is not affected other than by the addition of random noise.

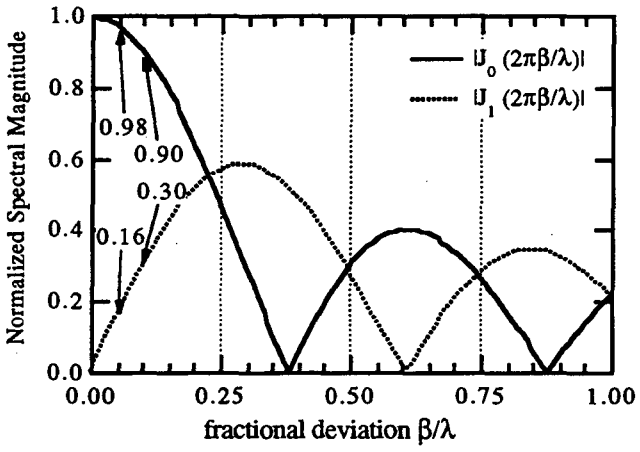

Figure 1

Main peak and 1st side-band magnitudes vs. amplitude of periodic position error. The effect of periodic position errors is to create sidebands of each peak whose magnitudes vary with the maximum position error. As illustrated, an error of 10% of the wavelength of the main line leads to a 10% loss in amplitude to the side bands.

author: E. J. Moler, submitted to APPLIED OPTICS, Optical Technology Division

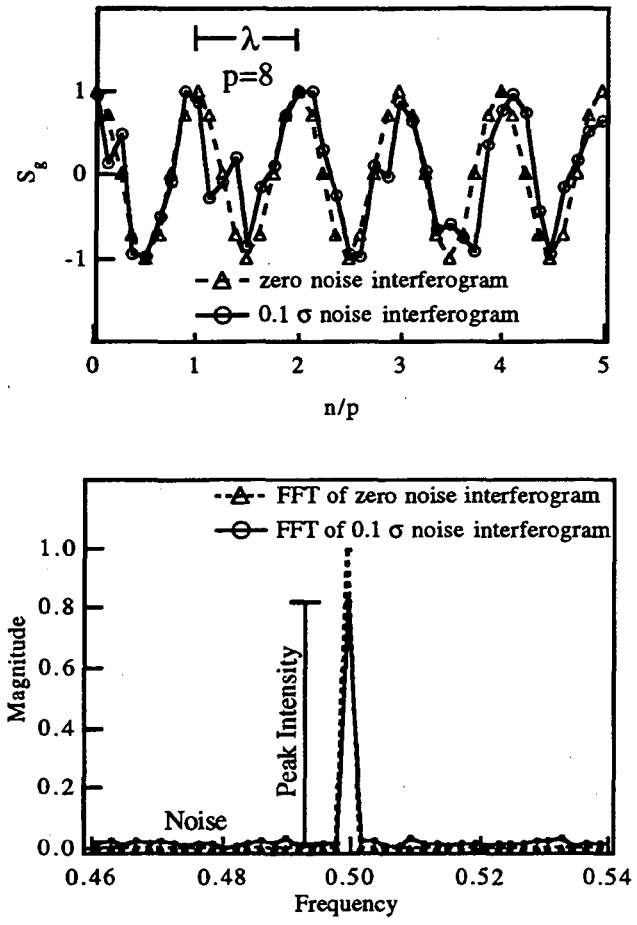

Figure 2

Interferograms, with and without position noise in sampling, and their FFT's. The sample rate is 8 points/period and 256 periods were included (but not shown).

author: E. J. Moler, submitted to APPLIED OPTICS, Optical Technology Division

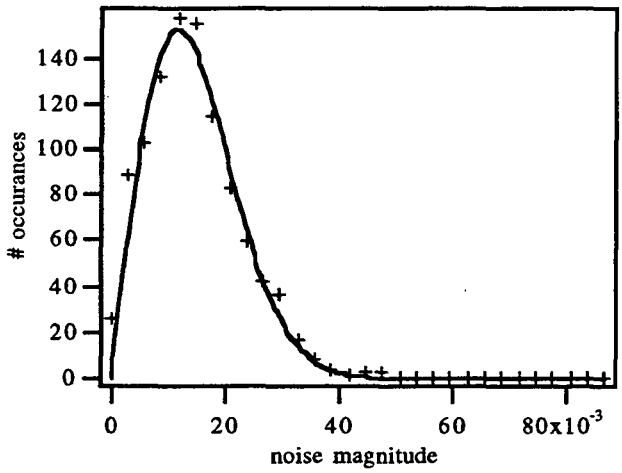

Figure 3

Histogram of noise amplitudes in the FFT. The solid line is a Rayleigh distribution, which fits as expected.

author: E. J. Moler,; submitted to APPLIED OPTICS, Optical Technology Division

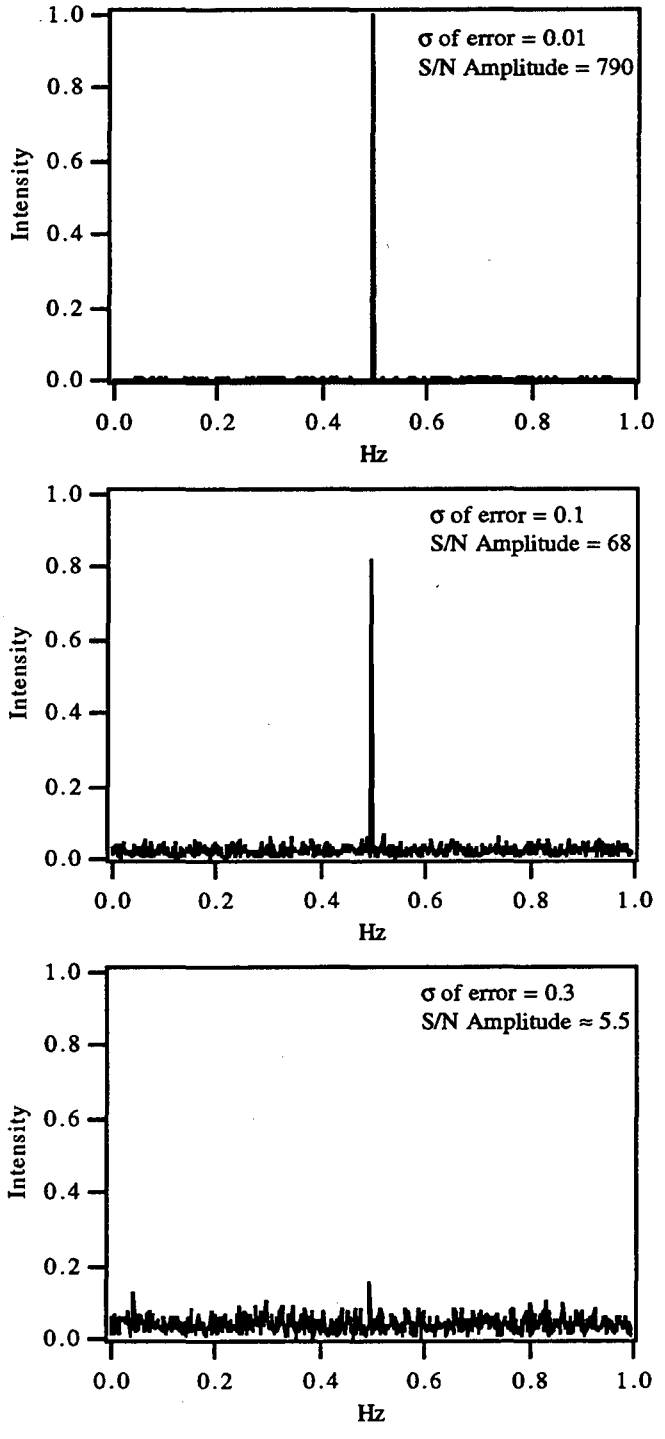

Figure 4

Simulated spectra with random position errors (σ) of 0.01, 0.1, and 0.3 of a period. Included are 256 periods with a sampling rate of 4 points/cycle. The signal/noise amplitude ratio is shown for each (see text for calculation method).

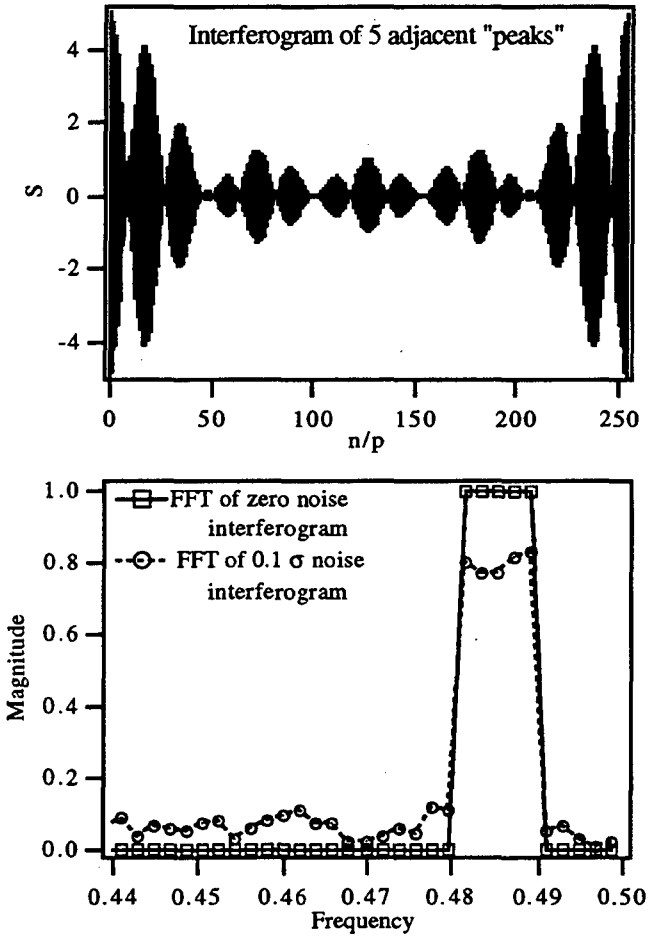

Figure 5

Interferogram of 5 component "peak" with noise and its FFT. Only the envelope of the interferogram is visible. The lineshape in the FFT is not affected other than by the addition of random noise.

author: E. J. Moler, submitted to APPLIED OPTICS, Optical Technology Division

LAWRENCE BERKELEY LABORATORY
UNIVERSITY OF CALIFORNIA
TECHNICAL INFORMATION DEPARTMENT
BERKELEY, CALIFORNIA 94720